

Trend for the multilayer relaxation sequence of stepped Cu surfaces

Juarez L. F. Da Silva,* Kurt Schroeder, and Stefan Blügel

Institut für Festkörperforschung, Forschungszentrum Jülich, D-52425 Jülich, Germany

(Received 23 May 2004; revised manuscript received 7 September 2004; published 29 December 2004)

We investigate suggested multilayer relaxation trends for the stepped metal surfaces by performing density-functional theory calculations, within the generalized gradient approximation and employing the all-electron full-potential linearized augmented plane wave (FLAPW) method, for stepped Cu surfaces. We found that the atom-rows trend, which correlates the multilayer relaxation sequence of stepped metal surfaces with the number of atom rows in the terrace, is not as general as has been assumed. While it holds true for closed stepped surfaces it does not apply for more open surfaces such as for Cu(320) and Cu(410). For example, we found relaxation sequences like $----+---$ for both surfaces, instead of the expected $--+---$ and $---+---$, respectively. The $-$ and $+$ signs indicate contraction and expansion, respectively, of the interlayer spacing. Our results show that the relaxation sequence of eleven stepped Cu surfaces, namely, (110), (311), (331), (211), (511), (210), (221), (711), (911), (410), and (320), follows the nearest-neighbor coordination trend, which correlates the relaxation sequence of the topmost interlayer spacings with the nearest-neighbor coordination number of the topmost surface atomic layers. Therefore, the reduction of the atomic coordination plays a stronger role in the relaxation sequences of stepped metal surfaces than the number of atoms exposed to the vacuum region.

DOI: 10.1103/PhysRevB.70.245432

PACS number(s): 68.47.De, 82.45.Jn, 71.15.Ap

I. INTRODUCTION

A microscopic understanding of many physical and chemical processes which take place at solid surfaces such as heterogenous catalysis, electrochemistry, corrosion, lubrication, etc., requires as a prerequisite an atom level understanding of surface defects like adatoms, vacancies, kinks, atomic steps, etc. (for reviews, see Ref. 1). In particular, atomic steps are always present on real solid surfaces, and hence, there is a clear interest to understand their atomic structure. To reach that goal, the study of high-Miller-index surfaces (vicinal or stepped), which have a periodic distribution of atomic steps separated by terraces of a low-Miller-index orientation (see Fig. 1), is the most simple and convenient approach.²

Most of the studies of the atomic structure of stepped metal surfaces using quantitative low-energy electron diffraction (LEED) intensity analysis,³⁻¹² semiempirical calculations,¹³⁻²² and first-principles calculations,²³⁻³¹ have been focused in obtaining an improvement in the understanding of the multilayer relaxation phenomenon. Based on a few of those results, Tian *et al.*⁷ suggested that there is a correlation between the interlayer relaxation-sequence of the topmost interlayer spacings and the number of atom-rows in the terrace of a stepped metal surface.

For a stepped metal surface with n atom-rows in the terrace exposed directly to the vacuum region, the topmost $n-1$ interlayer spacings ($d_{12}, \dots, d_{n-1,n}$) contract compared with the unrelaxed interlayer distances, while the n th and $(n+1)$ th interlayer spacings, i.e., $d_{n,n+1}$ and $d_{n+1,n+2}$, expand and contract, respectively. From now, contraction and expansions of the interlayer spacings are indicated by the sign $-$ and $+$, respectively. The correlation between the interlayer relaxation-sequences and the number of atom rows in the terrace has been understood by the *physical picture*,³²

which relates the contraction of the topmost layers exposed to the vacuum to the Smoluchowski charge smoothing of the electron density.³³

Furthermore, in a recent work, Sun *et al.*^{11,30} suggested that the multilayer relaxation sequences of the topmost interlayer spacings of a stepped metal surfaces correlates with the number of nearest neighbors of all atoms with coordination smaller than those in the bulk. In the process of multilayer relaxation, the interlayer spacing between each pair of layers with coordination smaller than in the bulk contracts. Sun

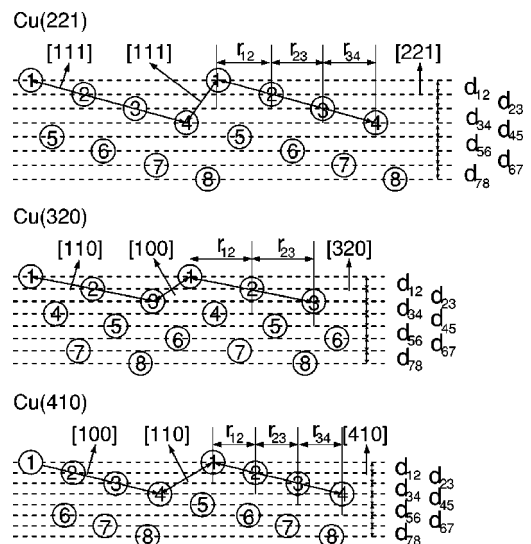


FIG. 1. Schematic side view of the unrelaxed stepped (221), (320), and (410) Cu surfaces. The Cu atoms are indicated by large open circles and the numbers inside it indicate the surface layers (increasing for deeper layers). The direction normal to the surfaces, terraces, and steps are indicated. The interlayer and registry distances are also indicated.

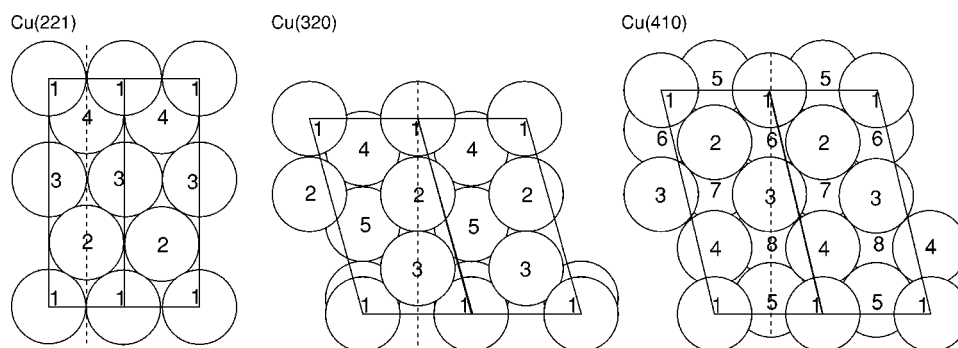


FIG. 2. Schematic top view of the stepped (221), (320), and (410) Cu surfaces. The Cu atoms are indicated by spheres with radius of half of the first-neighbors distance and the numbers inside it indicate the surface layer number (increasing for deeper layers). The (1×1) surface unit cell are indicated by solid lines, while the dashed lines indicate the mirror plane symmetry.

et al.^{11,30} proposed that this trend is also consistent with the Smoluchowski's concept of charge smoothing.³³

The most difficult problem in identifying trends for the multilayer relaxations for the topmost interlayer spacings of solid surfaces is the discrepancy between the published results. Several discrepancies with the multilayer relaxation trends described above have been reported. For example, a quantitative LEED intensity analysis study performed by Tian *et al.*⁷ and first-principle calculations performed by Geng and Freeman²⁴ for Cu(331), which has three atom-rows in the terrace, obtained a multilayer relaxation-sequence such as $-+-\dots$ instead of the expected $--+\dots$. However, recent first-principles calculations performed by Heid *et al.*,²⁶ Sun *et al.*,³⁰ and Da Silva *et al.*²⁸ found the expected multilayer relaxation-sequence from both trends, i.e., $--+\dots$ for Cu(331).

Independent first-principles calculations performed by Spišák²⁵ and by Heid *et al.*²⁶ for Cu(911), which has five atom-rows in the terrace, obtained a relaxation-sequence like $-+-+\dots$ and $--+\dots$, respectively, which are not the expected multilayer relaxation-sequence, i.e., $-----+\dots$. However, recent first-principle calculations performed by Da Silva *et al.*²⁹ found the expected relaxation-sequence for Cu(911).

Sklyadneva *et al.*,²⁰ using the embedded-atom method (EAM), studied a large number of stepped metal surfaces including the Cu(221) surface, which has four atom-rows in the terrace. Sklyadneva *et al.*²⁰ found $--+-$ for the interlayer relaxation-sequence, instead of the expected $-----+\dots$. However, they obtained the expected trend for Al(221) and Pd(221), which are geometrically similar to the Cu(221) surface. From our knowledge, there is no available quantitative LEED intensity analysis or first-principles calculations for this surface to clarify the unexpected behavior of the Cu(221) surface.

A quantitative LEED intensity analysis study of Cu(320), which has three atom-rows in the terrace, was performed by Tian *et al.*⁸ They found an interlayer relaxation-sequence like $--+$, which follows the atom-rows trend. This result was confirmed by Durukanoğlu and Rahman²¹ ($--+-$) using the EAM. However, a relaxation-sequence like $-----+\dots$ is expected from the nearest-neighbors coordination trend.³⁰ Recent first-principles all-electron calculations performed by Yamaguchi *et al.*³¹ found $-----+\dots$

for Cu(320), which is not in agreement with the results obtained by quantitative LEED and EAM calculations. Thus, the multilayer relaxation-sequence of Cu(320) is unclear.

To obtain a further understanding of the multilayer relaxation-sequence phenomenon on stepped metal surfaces, we performed density-functional theory (DFT) calculations employing the all-electron full-potential linearized augmented plane-wave (FLAPW) method for the stepped (221), (320), (410) Cu surfaces. As can be seen in Figs. 1 and 2, the (320) and (410) Cu surfaces are more open surfaces than Cu(221) and other stepped Cu surfaces previously studied by us.^{28,29} Hence, these surfaces can be considered as an important test for the suggested atom-rows and nearest-neighbors trends. Furthermore, we expect to contribute to the clarification of the discrepancies between the results obtained by semiempirical calculations, first-principle calculations, and quantitative LEED intensity analysis.

This paper is organized as follows: In Sec. II, the theoretical approach and the computational details are described. In Sec. III, we present and discuss our results for the multilayer relaxations of the Cu(320), Cu(221), and Cu(410) surfaces. Section IV summarizes the main conclusions obtained in the present work, while in the Appendix we report the most important test calculations.

II. METHOD AND COMPUTATIONAL DETAILS

Our theoretical calculations are based on DFT^{34,35} within the generalized gradient approximation.³⁶ The Kohn-Sham equations are solved using the all-electron FLAPW method,³⁷ as it is implemented in the FLEUR code,³⁸ in which solid surfaces are modelled using the film geometry proposed by Krakauer *et al.*,³⁹ i.e., a single slab sandwiched between two semi-infinite vacua. The LAPWs wave functions in the interstitial region are represented using a plane-wave expansion truncated to include only plane waves that have kinetic energies less than $K^{wf}=16.00$ Ry, and for the potential representation in the interstitial region, plane waves up to $G^{pot}=273$ Ry are considered. Inside the muffin-tin spheres with radius $R_{mt}=1.16$ Å, the wave functions are expanded in radial functions times spherical harmonics up to $l_{max}=9$, and for the potential a maximum of $\tilde{l}_{max}=9$ is also used. For the evaluation of the nonspherical matrix elements

TABLE I. Lattice parameters of the (1×1) surface unit cell for the (221), (320), and (410) Cu surfaces. $|\vec{a}|$ and $|\vec{b}|$ are the dimensions of the surface unit cell, while θ is the angle between the vectors \vec{a} and \vec{b} . d_0 is the interlayer spacing distance between two adjacent surface layers parallel to the surface of the ideal unrelaxed surface, while r_0 is the registry distance of the ideal unrelaxed surface along the direction perpendicular to the steps. All quantities, except the angle, are in units of the lattice constant. The experimental and theoretical Cu lattice constants are 3.61 Å and 3.63 Å, respectively.

	Cu(221)	Cu(320)	Cu(410)
$ \vec{a} $	$\sqrt{2}/2$	1	1
$ \vec{b} $	$\sqrt{18}/2$	$\sqrt{14}/2$	$\sqrt{18}/2$
θ	90°	105.501°	103.633°
d_0	$1/\sqrt{36}$	$1/\sqrt{52}$	$1/\sqrt{68}$
r_0	$5\sqrt{18}/36$	$5\sqrt{13}/26$	$4\sqrt{17}/34$

of the Hamiltonian we include terms up to $l_{max}^{ns}=6$.

Integrations over the surface Brillouin zone were performed using a two-dimensional Monkhorst-Pack \mathbf{k} -mesh,⁴⁰ namely, (14×5) , (10×5) , and (10×5) , for the (221), (320), and (410) Cu surfaces, respectively. The (221), (320), and (410) Cu surfaces were modelled using a (1×1) surface unit-cell, in which there is one Cu atom per surface layer. The most important geometric parameters of the (1×1) surface unit-cell are summarized in Table I. The theoretical equilibrium lattice constant, $a_0=3.63$ Å, which is used in our calculations was obtained by a fitting to Murnaghan's equation of state,⁴¹ which is in good agreement with experiments⁴² ($a_0=3.61$ Å).

The atomic positions of the surface atoms are determined by force minimization, in which the equilibrium configuration of the surface atoms is assumed when the atomic force on each atom is smaller than 0.50 mRy/a.u.. Further computational details can be found elsewhere,^{28,29} where the multilayer relaxations of the (111), (100), (110), (210), (211), (331), (311), (511), (711), and (911) Cu surfaces were studied.

III. RESULTS AND DISCUSSION

A high-Miller-index surface, which is also called a stepped or vicinal surface, consists of a periodic succession of terraces of a low-Miller-index orientation with a finite number of atom-rows exposed to the vacuum region separated by monoatomic steps (see Fig. 1). The Miller indices notation is not very convenient to be used in the study of high-Miller-index surfaces, e.g., Cu(320), because it does not indicate, at first sight, the geometrical structure of the surface. In order to make the structure of a stepped surface immediately obvious, the high-Miller-index surfaces such as Cu(320) can be represented in terms of the low-Miller-index orientation using the terrace-step notation, i.e., $n(hkl) \times (uvw)$, where n gives the width of the (hkl) terraces in term of the number of atom-rows exposed to the vacuum

region, and $[uvw]$ indicates the direction normal to the steps.²

For example, using this notation, the (211), (320), (410) Cu surfaces are represented by $4(111) \times (111)$, $3(110) \times (100)$, and $4(100) \times (110)$, respectively. This notation allows to obtain a quite direct view of the geometric structure of the stepped surfaces, since it makes obvious that there are four, three, and four atom-rows in the terrace exposed to the vacuum region for the (221), (320), (410), Cu surfaces, respectively.

For stepped surfaces, the multilayer surface relaxations can be decomposed in atomic displacements perpendicular and parallel to the surface. For (221), (320), and (410), the atomic displacements parallel to the surface are allowed only along of the direction perpendicular to the steps due to the presence of the mirror symmetry plane perpendicular to the steps (see Fig. 2). The displacements parallel to the surfaces do not change the translational symmetry of the surface unit cell.

In the present work, the interlayer relaxations perpendicular to the surface are calculated with respect to the unrelaxed clean surface interlayer distance, d_0 . We define, $\Delta d_{i,i+1} = 100(d_{i,i+1} - d_0)/d_0$, where $d_{i,i+1}$ is the interlayer distance between two atomic layers obtained by total energy minimization. Similarly, the relaxations parallel to the surface, which are commonly called registry relaxations are given by $\Delta r_{i,i+1} = 100(r_{i,i+1} - r_0)/r_0$, where $r_{i,i+1}$ is the registry distance along the direction perpendicular to the steps, as indicated in Fig. 1. The ideal interlayer and registry distances, d_0 and r_0 , respectively, are summarized in Table I.

The stepped Cu surfaces were modelled using from 13 up to 27 layers in the slab. For each surface, calculations were performed using at least two different number of layers in the slab, N_l , to check the convergence of the multilayer relaxations with respect to the number of layers in the slab. The results obtained for the multilayer relaxations, $\Delta d_{i,i+1}$ and $\Delta r_{i,i+1}$, are summarized in Table II, along with previously published results.

We found that 13 layers in the slab are sufficient to obtain a qualitative description of the multilayer relaxation-sequence for (221), (320), and (410) Cu surfaces, i.e., the interlayer relaxation-sequence does not change for $N_l > 13$. However, for a high precision quantitative description of the multilayer relaxations one needs more than 13 layers. We found that the registry relaxations do not play a decisive role in the multilayer relaxation-sequence. However, the registry relaxations change the magnitude of the interlayer relaxations. From now, we will discuss the results for each particular surface using results obtained with the largest number of layers in the slab.

A. Stepped Cu(221) surface

For Cu(221), which is schematically represented in Figs. 1 and 2, we found a multilayer relaxation-sequence like $---+---$. Therefore, our result is not in agreement with the results obtained by Sklyadneva *et al.*²⁰ $(-+--)$ using the EAM. For example, we found a contraction and an expansion for d_3 and d_5 , respectively, while Sklyadneva

TABLE II. Interlayer relaxations, $\Delta d_{i,i+1}$, respectively, of the (221), (320), and (410) Cu surfaces. N_i indicate the number of layers in the slab. $\Delta d_{i,i+1}$ are given with respect to the unrelaxed surface interlayer and registry distances, d_0 (see text and Table I). The + and - signs indicate expansion and contraction, respectively, of the interlayer and registry spacings.

Surf.	N_i	Reference	Δd_{12} (%)	Δd_{23} (%)	Δd_{34} (%)	Δd_{45} (%)	Δd_{56} (%)	Δd_{67} (%)	Δd_{78} (%)	Δd_{89} (%)	$\Delta d_{9,10}$ (%)
(221)	13	This work ^a	-13.82	-3.53	-2.05	+5.21	-5.18	+1.29			
	13	This work ^b	-13.43	-6.56	-5.15	+10.70	-4.96	+0.05			
	19	This work ^a	-14.97	-3.84	-0.96	+6.04	-4.55	-0.12	+1.51	-0.63	+0.27
	19	This work ^b	-16.91	-6.00	-2.31	+9.79	-5.65	+0.71	+0.82	-1.91	+1.32
		EAM (Ref. 20)	-10.9	-6.8	+6.0	-1.0	-5.4				
(320)	13	This work ^a	-11.75	-14.32	-5.37	-3.85	+12.38	-4.28			
	13	This work ^b	-12.51	-14.44	-4.61	-4.58	+12.33	-3.72			
	19	This work ^a	-11.16	-15.49	-7.30	-2.12	+11.39	-1.12	-2.69	+0.54	-0.61
	19	This work ^b	-12.73	-16.12	-5.93	-3.73	+12.74	-2.33	-1.32	-0.72	-0.11
	27	This work ^a	-10.65	-14.15	-8.02	-3.14	+12.38	-0.37	-1.32	-0.55	-1.73
	27	This work ^b	-9.23	-17.07	-7.75	-3.42	+10.21	-2.21	-1.56	-1.63	+0.21
	21	FLAPW (Ref. 31)	-16.7	-13.8	-5.9	-7.1	+16.7	-4.6	-1.7	+0.5	-5.8
	72	EAM (Ref. 21)	-13.63	-9.19	+2.88	-8.78	+10.69	-6.07	-1.63		
	LEED (Ref. 8)	-24±6	-16±12	+10±6							
(410)	13	This work ^a	-14.77	-4.32	-12.83	-2.68	+10.45	-4.66			
	13	This work ^b	-12.96	-7.65	-14.77	-3.17	+16.05	-7.06			
	21	This work ^a	-14.12	-2.95	-11.35	-5.16	+6.84	-2.78	-1.94	+4.33	+0.33
	21	This work ^b	-9.65	-7.05	-16.46	-5.97	+14.39	-3.14	-2.82	+1.50	-0.57
	21	FLAPW (Ref. 31)	-16.9	-10.9	-7.3	-3.6	+8.5	-5.4	-2.3	+1.5	+0.3
	90	EAM (Ref. 19)	-12.67	-8.74	-11.63	+6.16	+9.16	-4.60	-5.54	-3.64	

^aOnly relaxations perpendicular to the surface were included in the force optimization, $\Delta r_{i,i+1}=0 \forall i$ and j .

^bRelaxations parallel and perpendicular to the surface were included in the force optimization.

et al. found the opposite. We want to point out once more that similar EAM calculations performed by Sklyadneva *et al.* for Al(221) and Pd(221), which are geometrically similar to the Cu(221) surface, found a relaxation-sequence like ---+--.

We found that $|\Delta d_{12}| > |\Delta d_{23}| > |\Delta d_{34}|$, as well as $|\Delta d_{45}| > |\Delta d_{56}| > |\Delta d_{67}|$ for the Cu(221) surface, however, this trend is not obtained for the (320) and (410) Cu surfaces (see below). The interlayer distance between the topmost surface atomic layer and the fourth surface atomic layer is given by $3a_0/\sqrt{36}=1.81 \text{ \AA}$ (see Fig. 1), which became 1.66 \AA after the surface relaxation. Hence, the stepped surface tends to become more flat, which is expected due to the reduction in the electron density corrugation.

It can be seen in Table II that there are large discrepancies in the magnitude of the interlayer relaxations between our results and those obtained by EAM calculations.²⁰ The comparison shows that the contraction of the topmost interlayer spacing is quite well reproduced by EAM calculations, however, the interlayer relaxations of the Cu atoms at the bottom of the step edges are poorly reproduced by the EAM calculations.

B. Stepped Cu(320) surface

For Cu(320), which is schematically represented in Fig. 1, we found a multilayer relaxation-sequence like ----+---, i.e., the topmost four interlayer spacings

contract, while the fifth and sixth interlayer spacings expand and contract, respectively (see Table II). The same result was found using 13, 19, and 27 layers in the slab with and without taking into account atomic displacements parallel to the surface. Furthermore, we found the same relaxation-sequence using different cutoff energies and different sets of \mathbf{k} -points (see Appendix). Thus, we are certain of the relaxation-sequence obtained for Cu(320).

A quantitative LEED intensity analysis study of Cu(320) performed by Tian *et al.*⁸ found that the first interlayer spacing contracts by $-24 \pm 6\%$, which is larger by almost a factor of two compared with our result. For the second interlayer spacing, they obtained a contraction of $-16 \pm 12\%$, which is in better agreement with our result. For the third interlayer spacing, they obtained an expansion of $+10 \pm 6\%$, while we obtained a contraction of similar magnitude. The relaxation of further inner interlayer spacings was not taken into account in their work. Hence, their relaxation-sequence is ---+, which is in clear disagreement with our result.

We found that the magnitude of the relaxation of the fifth interlayer spacing has similar magnitude of the topmost interlayer spacing, which indicates the importance of taking into account at least up to the sixth interlayer spacing in the quantitative analysis of the LEED intensities. From the results above, we can conclude that the agreement between our calculations and the LEED results obtained by *et al.*⁸ is far from satisfactory. A much better agreement between DFT and quantitative LEED is obtained for other stepped Cu

TABLE III. Registry relaxations, $\Delta r_{i,i+1}$, respectively, of the (221), (320), and (410) Cu surfaces. N_l indicate the number of layers in the slab. $\Delta r_{i,i+1}$ are given with respect to the unrelaxed surface interlayer and registry distances, r_0 (see text and Table I). The + and - signs indicate expansion and contraction, respectively, of the interlayer and registry spacings.

Surf.	N_l	Reference	Δr_{12} (%)	Δr_{23} (%)	Δr_{34} (%)	Δr_{45} (%)	Δr_{56} (%)	Δr_{67} (%)	Δr_{78} (%)	Δr_{89} (%)	$\Delta r_{9,10}$ (%)
(221)	13	This work	-1.78	-1.17	-1.43	+1.53	+1.42	-0.46			
	19	This work	-1.48	-1.14	-1.52	+1.89	+1.01	-0.37	-0.58	+0.67	-0.31
(320)	13	This work	-0.44	+0.13	+0.42	+0.11	-0.60	+0.26			
	19	This work	-0.23	-0.10	+0.63	+0.16	-1.21	+0.63	-0.35	+0.52	-0.07
	27	This work	-1.11	+0.13	+0.54	+0.23	-1.02	+0.41	-0.09	+0.20	+0.09
	21	FLAPW (Ref. 31)	-0.12	+0.06	+0.39	+0.18	-1.28	+0.64	-0.09	+0.15	+0.00
	72	EAM (Ref. 21)	-0.59	+0.43	+0.37	+0.60	-0.56	+0.15	-0.22		
(410)	13	This work	-2.47	-1.02	-0.13	-1.78	+2.60	+0.46			
	21	This work	-2.84	-0.69	-0.25	-1.78	+3.11	+1.19	-0.52	-0.73	-0.49
	21	FLAPW (Ref. 31)	-1.95	-0.54	-0.13	-1.48	+3.24	+0.46	-0.72	-0.47	-0.23
	90	EAM (Ref. 19)	-2.08	-1.61	-0.27	-0.30	+1.79	-0.06	+0.90		

surfaces,^{28,29} we expect that the present discrepancy motivates further quantitative LEED intensity analysis study for the Cu(320) surface.

Our relaxation-sequence found for Cu(320) is in excellent agreement down to the 9th interlayer distance with the all-electron FLAPW calculations performed by Yamaguchi *et al.*³¹ However, there are small discrepancies in the magnitude of the topmost interlayer relaxation (see Table II). Our results and those obtained by EAM calculations,²¹ are not in good agreement. Particularly, the magnitude of the interlayer relaxations involving Cu atoms at the bottom of the step edges are poorly reproduced by the EAM calculations.

C. Stepped Cu(410) surface

For Cu(410), which is schematically show in Fig. 1, we found a multilayer relaxation-sequence like $-----+-----$. This result was found using different number of layers in the slab, e.g., 13 and 21, and for different cutoff energies and number of \mathbf{k} points (see Appendix). Thus, as for the Cu(320) surface, we are certain of our results.

We found that the magnitude of the topmost interlayer contraction decreases by a large value due to the registry relaxations, which is also found for the fifth interlayer spacing. Such behavior was also found for almost *all* studied stepped Cu surfaces by all-electron FLAPW calculations,^{28,29} except for the Cu(320) surface, in which the interlayer relaxations almost do not change due to the registry relaxations (see Tables II and III).

Our relaxation-sequence is in excellent agreement with the all-electron FLAPW calculations recently reported by Yamaguchi *et al.*,³¹ however, there are discrepancies in the magnitude of the interlayer relaxations. For example, we found $|\Delta d_{34}| > |\Delta d_{12}|$ while they found the opposite. Furthermore, they found that the topmost interlayer contraction is the largest relaxation in absolute value, while we found it for Δd_{56} . Our convergence tests reported in Appendix show that our results are converged with respect to the cutoff energy and number of \mathbf{k} -points, hence, such discrepancies might be due to the optimization of the atomic forces.

Durukanoğlu and Rahman¹⁹ performed EAM calculations for Cu(410) and obtained $---+---$, which differs from our result in the sign of the fourth interlayer spacing. They found expansion and we found contraction. The agreement between our results and those obtained by EAM calculations for the magnitude of the interlayer relaxations is good for particular interlayer spacings, e.g., d_{45} , d_{67} , however, there are large discrepancies for the other interlayer spacings.

IV. MULTILAYER RELAXATION PHENOMENON

The multilayer relaxation-phenomenon will be discussed in the present section using our results obtained for the (221), (320), and (410) surfaces, as well as our previous all-electron FLAPW results obtained for other Cu surfaces.^{28,29} We want to point out that the aim of the present section is to provide a further understanding of the multilayer relaxation-phenomenon by testing the atom-rows⁷ and nearest-neighbors coordination^{11,30} trends using our results for the Cu surfaces. The multilayer relaxation-sequence of eleven Cu surfaces are summarized in Table IV, along with the number of atom-rows in the (hkl) terrace and the nearest-neighbors coordination sequence of the topmost atomic layers.

A. Atom-rows trend

The atom-rows trend (see introduction) relates the relaxation-sequence to the number of atom-rows in the terrace. It is explained in terms of the *physical* picture,³² which relates the topmost surface layer contraction to the Smoluchowski charge smoothing of the electron density.³³ On a real solid surface, electrons smooth and spread out mainly to lower their kinetic energy. This weakens the electron-density corrugation and means that the electron density spreads from the region above the atoms (on-top site region) to the region between them (hollow site region). Thus, electrostatic forces cause the topmost surface layers to move inwards resulting in a contraction of the topmost interlayer spacing. The *physical* picture does not take in account

TABLE IV. Multilayer relaxation and coordination sequences for Cu surfaces. The second column indicates the number of atom rows in the (hkl) terrace exposed to the vacuum region, which are separated by (uvw) steps. The fifth column indicates the sequence of coordination numbers [number of nearest-neighbors (NN)] for the outermost surface layers down to where the bulk fcc coordination (i.e., 12) is obtained. N_c indicates the number of surface layers for which the coordination is smaller than the bulk Cu coordination. The last column summarizes the multilayer relaxation sequence for several stepped Cu surfaces as calculated with the all-electron FLAPW method in the present work and in our previous work (Refs. 28 and 29).

Surface	Atom rows in the terraces	Terrace (hkl)	Step (uvw)	First-neighbors coordination sequence	N_c ($NN < 12$)	Multilayer relaxation sequence
Cu(110)	2			7, 11, 12, 12, ...	2	-+-...
Cu(311)	2	(100)	(111)	7, 10, 12, 12, ...	2	-+-...
Cu(331)	3	(111)	(111)	7, 9, 11, 12, 12, ...	3	--+...
Cu(211)	3	(111)	(100)	7, 9, 10, 12, 12, ...	3	--+...
Cu(511)	3	(100)	(111)	7, 8, 10, 12, 12, ...	3	--+...
Cu(210)	3	(110)	(100)	6, 9, 11, 12, 12, ...	3	--+...
Cu(221)	4	(111)	(111)	7, 9, 9, 11, 12, 12, ...	4	----+...
Cu(711)	4	(100)	(111)	7, 8, 8, 10, 12, 12, ...	4	----+...
Cu(911)	5	(100)	(111)	7, 8, 8, 8, 10, 12, 12, ...	5	----+...
Cu(410)	4	(100)	(110)	6, 8, 8, 9, 11, 12, 12, ...	5	----+...
Cu(320)	3	(110)	(100)	6, 7, 9, 11, 11, 12, 12, ...	5	----+...

the nature of the chemical bonding in the different metal surfaces, i.e., similar multilayer relaxation-sequence is expected for geometrically similar stepped metal surfaces.

For solid surfaces with a large electron-density corrugation such as fcc(110), the contraction of the topmost inter-layer spacing is larger than for closed-packed surfaces such as fcc(111), which is indeed obtained by LEED intensity analysis and first-principles calculations. For stepped surfaces several atom-rows on the terraces (which belong to different planes) are exposed to the vacuum region. These atoms are affected by the Smoluchowski charge smoothing of the electron-density, and hence, a contraction is obtained for the surface atoms exposed to the vacuum. As the atom-rows exposed to the vacuum belong to different surface layers, a contraction is observed for several surface layers, which depends on the number of atom-rows in the terrace. Thus, it explains the atom-rows trend.

We found that the multilayer relaxation-sequence of the (110), (311), (331), (211), (511), (210), (221), (711), and (911) Cu surfaces follows the atom-rows trend, however, the same was not found for (320) and (410) (see Table IV). For example, the (410) and (320) Cu surfaces have four and three atom-rows in the terraces, hence, according to the atom-rows trend, it is expected relaxation-sequences like $---+---$ and $--+---$, respectively. However, we found a multilayer relaxation-sequence like $----+---$ for both surfaces, which is expected for a stepped surface with five atom-rows in the terrace such as for Cu(911). Therefore, the (410) and (320) Cu surfaces have an irregular behavior with respect to the atom-rows trend, i.e., the relaxation-sequence does not correlate with the number of atom-rows in the terrace.

To understand such irregular behavior for (320) and (410), a top view of these surfaces are required, as pointed out by previous work.³¹ It can be seen in Fig. 2 that the Cu atoms numbered by 4 and 5 are also exposed to the vacuum region.

However, these atoms are below the terrace, as can be seen in Fig. 1. Thus, for (320), the relaxation-sequence correlates with the number of Cu atoms exposed to the vacuum region and not with the number of atom-rows in the terrace.

For Cu(410), the Cu atoms in the topmost eight atomic layers are exposed to the vacuum region (see Fig. 2). The Cu atoms numbered from 1 up to 4 are in the terrace, while from 5 up to 8 are below the terrace. Using the same procedure used for Cu(320), i.e., taken into account the surface atoms exposed to the vacuum region, we would expect a relaxation-sequence like $-----+---$, however, we found $----+---$ from our calculations. Thus, the relaxation-sequence found for Cu(410) does not correlate with the number of atom-rows or surface atoms exposed to the vacuum region. Therefore, the atom-rows trend is not general enough to explain and predict the perpendicular multilayer relaxation-sequence of stepped metal surfaces.

B. Nearest-neighbor coordination trend

Sun *et al.*^{11,30} suggested that the nearest-neighbor coordination trend is consistent with the Smoluchowski's concept of charge smoothing.³³ However, we want to point out that the nearest-neighbor coordination trend is a simple consequence of the chemist's concept of bond-order bond-length correlation,⁴⁴ which correlates the contraction of the topmost surface layer to the reduction of coordination of the surface atoms. This concept has also been known as *chemical picture*.⁴³

In the chemist's concept the principle is the saturation of valence. Every atom has a fixed number of valence electrons, e.g., 11 for Cu. Hence, in the bulk Cu eleven electrons are distributed in 12 bondings. If a surface is formed, the surface atoms lose several neighbors. The electrons that were involved in the bonding to these neighbor atoms redistribute themselves in the remaining bonds, i.e., to the atoms in the

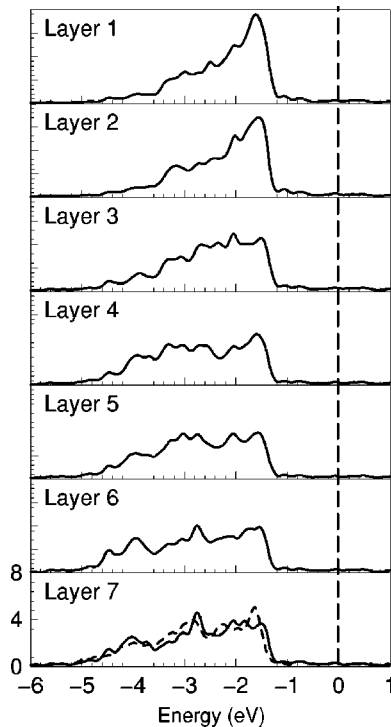


FIG. 3. Local density of states (LDOS) of the Cu(320) surface calculated for the topmost seven atomic layers. The vertical dashed line indicates the Fermi energy. The dashed line in the bottom panel indicates the LDOS of bulk Cu. All plots are on the same scale.

surface layer below. Thus, the number of electrons per bond increases, which reduces the bond length, i.e., the interlayer distance between the surface layers.

Furthermore, as an effect of the reduction of the coordination number, there are large changes in the density of states of the surface atoms. In Fig. 3, we plotted the local density of states (LDOS) for the Cu(320) surface for the topmost seven surface layers. There is a large decrease in the bandwidth of the LDOS for the topmost surface layer. The changes in the LDOS are not restricted to the topmost three surface atomic layers, which are exposed directly to the vacuum region, but extend for inner surface layers. It can be seen in Table IV that the coordination of the topmost seven surface layers are 6, 7, 9, 11, 11, 12, and 12, respectively. Thus, it explains the similar shape of the LDOS for the topmost two surface layers, as well as for the layers numbered by 4 and 5. The LDOS approaches that of bulk Cu only for the sixth and seventh surface layer (see Fig. 3).

We calculated the number of nearest-neighbors coordination for every atomic layer down to the plane where we obtain the bulk Cu coordination Cu, i.e., 12. The number of nearest-neighbors were obtained for the ideal unrelaxed surface and the results are summarized in Table IV. For example, for Cu(110), the bulk coordination number is obtained for the third atomic layer, while for Cu(911), it is obtained only for the sixth atomic layer. We can see in Table IV that there is a clear correlation between the number of surface atomic layers in which the coordination is smaller than the bulk coordination and the multilayer relaxation-

sequence, which include all studied Cu surfaces. Therefore, all studied surfaces follow the nearest-neighbor coordination trend, which does not occur with the atom-rows trend.

The nearest-neighbor coordination trend can be written in the following: For an ideal stepped metal surface, in which the topmost n surface atomic layers have nearest-neighbor coordination numbers smaller than the bulk coordination (12 for face-centered cubic structure), the topmost $n-1$ interlayer spacing contracts compared with the ideal unrelaxed surface, while the n th interlayer spacing expands and the $(n+1)$ th contracts, respectively. For example, for Cu(711), the coordination of the Cu atoms in the topmost five surface atomic layers are 7, 8, 8, 10, and 12, respectively. There are four surface layers in which the coordination numbers are smaller than the bulk coordination, and the relaxation-sequence is $---+---$.

We noted from Table IV that the atom-rows trend is a particular case of the nearest-neighbor coordination trend, hence, *all* stepped metal surfaces with fcc structure that fit in the atom-rows trend also fit in the nearest-neighbor coordination trend. Thus, it is a clear evidence that the coordination trend is more general than the atom-rows trend. Whether the coordination trend found based on calculations for fcc Cu also holds true for other crystal structures, e.g., body-centered cubic, remains to be tested. We want to point out that the both trends do not take into account the nature of the chemical bonding in the different metals, since it only uses the coordination numbers and number of atom-rows, which are the same for all metals with the same atomic structure.

V. SUMMARY

In the present work we performed DFT calculations employing the all-electron FLAPW method for the stepped (221), (320), and (410) Cu surfaces. Based on the results obtained for the mentioned Cu surfaces and from our previous FLAPW calculations for other stepped Cu surfaces,^{28,29} we investigated previous suggested multilayer relaxation-sequence trends,^{7,11,30} e.g., atom-rows and nearest-neighbor coordination trends, for stepped metal surfaces.

We found that the multilayer relaxation-sequence of eleven stepped Cu surfaces, namely, (110), (311), (331), (211), (511), (210), (221), (711), (911), (410), (320), follows the nearest-neighbor coordination trend,^{11,30} which is not true for the atom-rows trend.⁷ E.g., from the atom-rows trend, it is expected multilayer relaxation-sequences like $---+---$ and $---+---$ for Cu(320) and Cu(410), respectively, however, we found $----+---$ for both surfaces. Therefore, based on first-principles calculations for stepped Cu surfaces, we found that the nearest-neighbor coordination trend is the most general trend to predict and explains the multilayer relaxation-sequence of the topmost interlayer spacings of stepped Cu metal surfaces.

The nearest-neighbor coordination trend can be rewritten as follows: For a stepped metal surface, in which the topmost n surface atomic layers have nearest-neighbor coordination smaller than for the bulk crystal (calculated for the ideal unrelaxed surfaces), the topmost $(n-1)$ interlayer spacings, i.e., $(d_{12}, \dots, d_{n-1,n})$, contract compared with the unrelaxed

TABLE V. Interlayer and registry relaxations, $\Delta d_{i,i+1}$ and $\Delta r_{i,i+1}$, respectively, of the (320) and (410) Cu surfaces as a function of the cutoff energy, K^{wf} , and to the number of \mathbf{k} points in the surface Brillouin zone (BZ), $N_{\text{BZ}}^{\mathbf{k}}$. The $-$ and $+$ signs indicate contraction and expansion, respectively, of the interlayer and registry spacings. $N_{\text{BZ}}^{\mathbf{k}}=4, 9, 16, 25, 36,$ and 49 correspond to the $(4 \times 2), (6 \times 3), (8 \times 4), (10 \times 5), (12 \times 6),$ and (14×7) two-dimensional Monkhorst-Pack \mathbf{k} -point meshes, respectively.

Surf.	K^{wf} (Ry)	$N_{\text{BZ}}^{\mathbf{k}}$	Δd_{12} (%)	Δd_{23} (%)	Δd_{34} (%)	Δd_{45} (%)	Δd_{56} (%)	Δd_{67} (%)	Δr_{12} (%)	Δr_{23} (%)	Δr_{34} (%)	Δr_{45} (%)	Δr_{56} (%)	Δr_{67} (%)
(320)	10.56	25	-14.44	-17.72	-5.54	-10.16	+13.27	-7.16	-1.03	+0.62	-0.07	+0.08	-1.08	+0.17
	12.25	25	-13.35	-15.66	-4.33	-7.77	+12.95	-4.92	-0.72	+0.37	+0.25	+0.18	-0.68	+0.26
	14.06	25	-12.98	-14.93	-3.91	-6.49	+13.27	-4.50	-0.56	+0.26	+0.33	+0.19	-0.59	+0.29
	16.00	25	-12.51	-14.44	-4.61	-4.58	+12.33	-3.72	-0.44	+0.13	+0.42	+0.11	-0.60	+0.26
	18.06	25	-12.96	-14.33	-3.54	-5.77	+13.49	-3.87	-0.44	+0.17	+0.42	+0.18	-0.53	+0.29
	20.25	25	-12.78	-14.28	-3.58	-5.46	+13.22	-3.61	-0.43	+0.15	+0.45	+0.19	-0.54	+0.30
(320)	16.00	4	-7.29	-16.73	-4.80	-2.33	+9.47	-2.69	-1.02	+0.99	-0.05	+0.42	-0.69	-0.37
	16.00	9	-12.82	-14.65	-4.63	-6.22	+14.41	-4.39	-0.61	+0.34	+0.29	+0.36	-0.68	+0.24
	16.00	16	-13.96	-14.65	-5.00	-7.54	+15.45	-4.26	-0.43	+0.20	+0.45	+0.08	-0.68	+0.29
	16.00	25	-12.51	-14.44	-4.61	-4.58	+12.33	-3.72	-0.44	+0.13	+0.42	+0.11	-0.60	+0.26
	16.00	36	-13.14	-14.81	-4.49	-6.08	+13.36	-3.31	-0.38	+0.12	+0.48	+0.12	-0.68	+0.26
	16.00	49	-13.44	-14.74	-4.47	-6.36	+13.65	-3.36	-0.40	+0.10	+0.47	+0.15	-0.65	+0.22
(410)	10.56	25	-11.92	-7.99	-18.87	-9.73	+16.71	-10.14	-3.80	-0.94	+1.21	-2.08	+2.34	+0.72
	12.25	25	-13.15	-8.76	-16.81	-4.30	+16.78	-9.10	-3.15	-1.11	+0.50	-1.78	+2.42	+0.54
	14.06	25	-13.10	-7.91	-15.52	-3.33	+16.31	-7.64	-2.74	-1.03	+0.09	-1.66	+2.44	+0.47
	16.00	25	-12.96	-7.65	-14.77	-3.17	+16.05	-7.06	-2.47	-1.02	-0.13	-1.78	+2.60	+0.46
	18.06	25	-12.99	-8.14	-15.46	-1.38	+16.90	-7.80	-2.53	-1.12	-0.09	-1.64	+2.53	+0.45
	20.25	25	-12.82	-8.08	-15.40	-1.42	+16.87	-7.53	-2.53	-1.12	-0.12	-1.63	+2.51	+0.46
(410)	16.001	4	-12.71	-6.34	-16.33	-4.50	+16.39	-7.71	-2.95	-1.62	+0.21	-1.31	+2.54	+0.75
	16.00	9	-11.87	-8.10	-13.30	-3.74	+15.66	-6.98	-3.13	-0.81	+0.40	-1.60	+2.12	+0.45
	16.00	16	-12.81	-8.81	-15.18	-2.61	+16.11	-6.81	-2.61	-0.96	-0.07	-1.70	+2.52	+0.43
	16.00	25	-12.96	-7.65	-14.77	-3.17	+16.05	-7.06	-2.47	-1.02	-0.13	-1.78	+2.60	+0.46
	16.00	36	-12.52	-8.37	-14.89	-2.37	+15.40	-7.40	-2.57	-1.04	+0.01	-1.61	+2.38	+0.47
	16.00	49	-12.29	-8.96	-15.01	-1.94	+15.83	-7.81	-2.51	-1.08	+0.02	-1.53	+2.39	+0.43

interlayer spacing, while the n th and $(n+1)$ th interlayer spacings, i.e., $d_{n,n+1}$ and $d_{n+1,n+2}$, expand and contract, respectively. In the present work, we explain this trend as a simple consequence of the chemist's concept of bond-order bond-length correlation.⁴⁴

We expect that future first-principles calculations and quantitative LEED intensity analysis for stepped metal surfaces geometrically similar to the (320) and (410) Cu surfaces find a similar trend as obtained by us, i.e., the atomrows trend is not valid for more open stepped metal surfaces.

ACKNOWLEDGMENTS

We would like to thank G. Bihlmayer for his help with the FLEURwin 0 code.

APPENDIX

Here, we report and discuss the dependence of the magnitude of the interlayer and registry relaxations of the (320) and (410) Cu surfaces with respect to computational param-

eters such as the cutoff energy, K^{wf} , and number of \mathbf{k} -points in the surface BZ, $N_{\text{BZ}}^{\mathbf{k}}$, used to perform the integration over the BZ. We want to point out that these tests were performed to check carefully the relaxation-sequence obtained for Cu(320) and Cu(410), i.e., $-----+-----$, as well as the magnitude of the interlayer relaxations, which differ from previously published studies.^{8,19,21,31}

The interlayer and registry relaxations calculated using a slab with 13 layers are close to the results obtained using slabs with a higher number of layers, e.g., 19 (see Table II). Thus, our test calculations were performed using 13 layers in the slab. Calculations were performed for cutoff energies from 10.56 Ry up to 20.25 Ry and for \mathbf{k} -points from $N_{\text{BZ}}^{\mathbf{k}}=4$ up to 49. All results are summarized in Table V.

We found that the interlayer relaxation-sequence for Cu(320) and Cu(410) is $-----+-----$ for *all* chosen cutoff energies and \mathbf{k} -point sets. Thus, our systematic test calculations show that the relaxation-sequence obtained in the present work is a real physical behavior for these surfaces and not a result of unconverged calculations. On the other hand, we found changes in the sign of the registry relaxations with increasing computational parameters such the cutoff en-

ergy, e.g., calculations for Cu(320) using $K^{wf}=10.56$ Ry found $-+-+--$ while for $K^{wf}=16.00$ Ry we found $-++++-$.

We found changes in the magnitude of the interlayer relaxations with increasing cutoff energy and number of \mathbf{k} -points, which is expected (see Table V). In particular, we found that some interlayer distance relaxations are strongly dependent on the computational parameters, e.g., d_{45} , while

there are only relatively small changes of the contraction of the topmost interlayer spacing. As can be seen in Table V, a cutoff energy of 16.00 Ry and 25 \mathbf{k} -points in the surface BZ provide well converged interlayer and registry relaxations for (320) and (410) Cu surfaces. Thus, the same cutoff energy and similar high quality \mathbf{k} -points were used in the calculations for the Cu(221) surfaces, as previously for other stepped Cu surfaces.^{28,29}

*Corresponding author. Email address: j.dasilva@fz-juelich.de

¹For a retrospective of surface science, see articles in Surf. Sci. **500**, 1–1053 (2002).

²M.-C. Desjonquères and D. Spanjaard, *Concepts in Surface Science* (Springer, Berlin, 1995).

³P. R. Watson and K. A. R. Mitchell, Surf. Sci. **203**, 323 (1988).

⁴S. R. Parkin, P. R. Watson, R. A. McFarlane, and K. A. R. Mitchell, Solid State Commun. **78**, 841 (1991).

⁵Y. P. Guo, K. C. Tan, A. T. S. Wee, and C. H. A. Huan, Surf. Sci. Lett. **6**, 819 (1999).

⁶Th. Seyller, R. D. Dohl, and F. Jona, J. Vac. Sci. Technol. A **17**, 1635 (1999).

⁷Y. Tian, K.-W. Lin, and F. Jona, Phys. Rev. B **62**, 12844 (2000).

⁸Y. Tian, J. Quinn, K.-W. Lin, and F. Jona, Phys. Rev. B **61**, 4904 (2000).

⁹S. Walter, H. Baier, M. Weinelt, K. Heinz and Th. Fauster, Phys. Rev. B **63**, 155407 (2001).

¹⁰Ismail, S. Chandravakar and D. M. Zehner, Surf. Sci. **504**, L201 (2002).

¹¹Y. Y. Sun, H. Xu, J. C. Zheng, J. Y. Zhou, Y. P. Feng, A. C. H. Huan, and A. T. S. Wee, Phys. Rev. B **68**, 115420 (2003).

¹²M. A. Albrecht, R. Blome, H. L. Meyerheim, W. Moritz, I. K. Robinson, and D. A. Walko (unpublished). The quantitative LEED intensity analysis results are reported in D. A. Walko and I. K. Robinson, Phys. Rev. B **59**, 15446 (1999).

¹³P. Jiang, F. Jona, and P. M. Marcus, Phys. Rev. B **35**, 7952 (1987).

¹⁴B. Loisel, D. Gorse, V. Pontikis, and J. Lapujoulade, Surf. Sci. **221**, 365 (1989).

¹⁵S. B. Sinnott, M. S. Stave, T. J. Raeker, and A. E. DePristo, Phys. Rev. B **44**, 8927 (1991).

¹⁶K. D. Hammonds and R. M. Lynden-Bell, Surf. Sci. **278**, 437 (1992).

¹⁷Z.-J. Tian and T. S. Rahman, Phys. Rev. B **47**, 9751 (1993).

¹⁸S. Durukanoğlu, A. Kara, and T. S. Rahman, Phys. Rev. B **55**, 13894 (1997).

¹⁹S. Durukanoğlu and T. S. Rahman, Surf. Sci. **409**, 395 (1998).

²⁰I. Y. Sklyadneva, G. G. Rusina, and E. V. Chulkov, Surf. Sci.

416, 17 (1998).

²¹S. Durukanoğlu and T. S. Rahman, Phys. Rev. B **67**, 205406 (2003).

²²H. Yildirim and S. Durukanoğlu, Surf. Sci. **557**, 190 (2004).

²³C. Y. Wei, Steven P. Lewis, E. J. Mele, and A. M. Rappe, Phys. Rev. B **57**, 10062 (1998).

²⁴W. T. Geng and A. J. Freeman, Phys. Rev. B **64**, 115401 (2001).

²⁵D. Spišák, Surf. Sci. **489**, 151 (2001).

²⁶R. Heid, K. P. Bohnen, A. Kara, and T. S. Rahman, Phys. Rev. B **65**, 115405 (2002).

²⁷F. E. Olsson and M. Persson, Surf. Sci. **540**, 172 (2003).

²⁸J. L. F. Da Silva, K. Schroeder, and S. Blügel, Phys. Rev. B **69**, 245411 (2004).

²⁹J. L. F. Da Silva, K. Schroeder, and S. Blügel, “First-principles investigations of the role of registry relaxations on stepped Cu(100) surfaces” (unpublished).

³⁰Y. Y. Sun, H. Xu, Y. P. Feng, A. C. H. Huan, A. T. S. Wee, Surf. Sci. **548**, 309 (2004).

³¹M. Yamaguchi, H. Kaburaki, and A. J. Freeman, Phys. Rev. B **69**, 045408 (2004).

³²M. W. Finnis and V. Heine, J. Phys. F: Met. Phys. **4**, L37 (1974).

³³R. Smoluchowski, Phys. Rev. **60**, 661 (1941).

³⁴P. Hohenberg and W. Kohn, Phys. Rev. **136**, B864 (1964).

³⁵W. Kohn and L. J. Sham, Phys. Rev. **140**, A1133 (1965).

³⁶J. P. Perdew, K. Burke, and M. Ernzerhof, Phys. Rev. Lett. **77**, 3865 (1996).

³⁷D. J. Singh, *Plane Waves, Pseudopotentials and LAPW Method* (Kluwer Academic, Boston, Dordrecht, London, 1994).

³⁸<http://www.flapw.de>.

³⁹H. Krakauer, M. Posternak, and A. J. Freeman, Phys. Rev. B **19**, 1706 (1979).

⁴⁰H. J. Monkhorst and J. D. Pack, Phys. Rev. B **13**, 5188 (1976).

⁴¹F. D. Murnaghan, Proc. Natl. Acad. Sci. U.S.A. **50**, 697 (1944).

⁴²C. Kittel, in *Introduction to Solid State Physics*, 7th ed. (Wiley, New York, 1996).

⁴³P. J. Feibelman, Phys. Rev. B **46**, 2532 (1992).

⁴⁴L. Pauling, *The Nature of the Chemical Bond*, 3rd ed. (Cornell University Press, Ithaca, NY, 1960).